Laboratori Nazionali di Frascati

LNF-68/32

M. Ladu, M. Pelliccioni, P. Picchi and G. Verri : A CONTRIBUTION TO THE SKYSHINE STUDY.

Estratto da : Nuclear Instr. and Meth. 62, 51 (1968)

NUCLEAR INSTRUMENTS AND METHODS 62 (1968) 51–56; © NORTH-HOLLAND PUBLISHING CO.

A CONTRIBUTION TO THE SKYSHINE STUDY

M. LADU, M. PELLICCIONI, P. PICCHI and G. VERRI

Laboratori Nazionali di Frascati del CNEN, Frascati, Italy

Received 29 January 1968

The results obtained by application of the Monte Carlo method to the skyshine study are described. We found that the neutron fluence ϕ per primary neutron decreases with distance r according to the laws $\phi(r) = Ar^{-\alpha}$ for distances between 20 m and 300 m, and $\phi(r) = B \exp(-r\lambda)$ for greater distances. The dependence of the coefficients A, B, α and λ, on a number of different parameters is studied. The results are compared with the Lindenbaum theory, and a good agreement is found. The effects of shields over the intensity and energy distribution of the diffused neutrons are also studied. Finally, the values of the back-scattering coefficient of the earth's surface is obtained.

1. Introduction

The term "skyshine radiation" or more shortly "skyshine" is used in physics to indicate the radiation, which coming from a source on the earth's surface and initially directed upwards, is scattered down by collisions with the nuclei of the air.

Particle accelerators, if missing an efficient upper shield, are important sources of skyshine. In this case, the effect is essentially due to the giant-resonance neutrons, of about 5 MeV energy, for which the diffusion cross sections in nitrogen and oxygen are great with respect to the capture cross sections.

These neutrons can considerably contribute to the dose near the great accelerators, and at great distances they constitute practically the main component of the dose.

A rigorous treatment of the skyshine is extremely difficult because of the numerous parameters and of the effect due to the earth's surface which, although having a greater capture cross section with respect to air, cannot be considered a perfect absorber because of its back scattering coefficient lying between 0.5 and 0.8 for neutrons of energy between 1 MeV and 10 MeV [1]).

Therefore the effect of the earth's surface cannot be neglected, because just there it is important to know the intensity and the energy of the radiation.

In spite of these difficulties, a semi-empirical theory in very good agreement with the experimental results has been formulated by Lindenbaum[2]).

We studied the problem by simulating the phenomenon with the Monte Carlo method in order to take strictly into account all the parameters and the effect of the earth's surface.

TABLE 1
Composition of the earth, corresponding to 30% water contents.

H	O	Na	Mg	Al	Si	K	Ca	Fe
3.3	60.8	2	1.5	5.8	19.7	1.8	2.6	3.6

2. Description of the computation

The computation has been performed considering an isotropic point source of 5 MeV neutrons, placed at the separation plane of two infinite media, the air and the earth.

A nitrogen 79% and oxygen 21% composition by weight has been assumed for the air.

For the earth the composition, corresponding to 30% water contents, is shown in table 1.

To study also the effect of lateral shields over the skyshine intensity we considered three cases. In the first, merely geometric, case the neutrons are emitted over the whole solid angle.

In the two other cases only neutrons emitted in cones of 30° and 60° semi-aperture, respectively, are considered. These last two cases correspond in practice to accelerators without overhead screen, but with efficient lateral shields.

The data used and physical processes are described in the next paragraph.

To express the results as neutron fluence, the separation plane has been divided into areas enclosed between concentric circles, with the centers on the source and the radii progessively increasing with a 20 m step.

Every time a neutron passes through the separation surface, the coordinates, the energy and the sense of crossing are registered.

The computation, programmed in FORTRAN IV language, has been performed on the IBM 7040 computer of the Istituto Superiore di Sanità in Rome.

To obtain a good statistics also at great distances from the source, about 20000 neutrons have been followed.

3. Physical data and processes

The physical processes considered are the following: elastic interactions, inelastic interactions, capture.

To compute the probability for these processes we

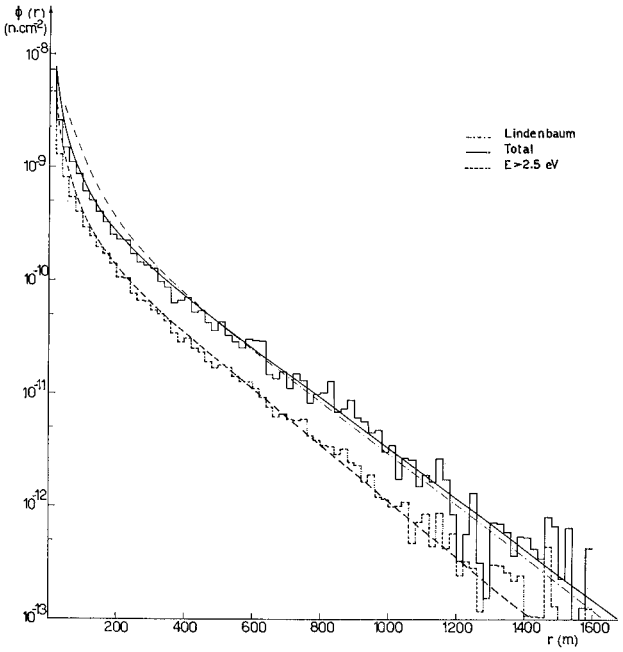

Fig. 1. Neutron fluence as a function of the distance from the source, with $\theta = 90°$.

used, for each of the elements involved, the experimental data on the total cross sections $\sigma_t(E)$ [3,4]), on the non-elastic cross sections $\sigma_n(E)$ [3,4]) and on the inelastic cross sections $\sigma_{n'}(E)$ [3,5,6]).

The character of the interaction is different according to whether the energy is greater or less than 0.2 eV.

3.1. $E > 0.2$ eV

When the energy of the neutron is greater than 0.2 eV we consider elastic interactions, inelastic interactions and capture.

Elastic scattering: The elastic scattering cross section $\sigma_{el}(E)$ was obtained from experimental data, from the relation:

$$\sigma_{el}(E) = \sigma_t(E) - \sigma_n(E).$$

The distribution of the scattering angle was also obtained from experimental data, using for each element the results of measures on differential cross sections[6,7]).

Only for hydrogen the angular distribution has been assumed isotropic[7]).

Inelastic scattering: The inelastic scattering has been assumed to be isotropic in the center of mass system[8]).

According to the statistical theory, the probability for a neutron of initial energy E_0 to be scattered into the energy range E_n to $E_n + dE_n$ is

$$dP(E_0, E_n) = (E_n/\theta^2)\exp(-E_n/\theta)dE_n,$$

where $\theta^2 = E_0/a$ and a is a parameter, whose values are given in table 2.

Because of their low atomic weight, nitrogen, oxygen

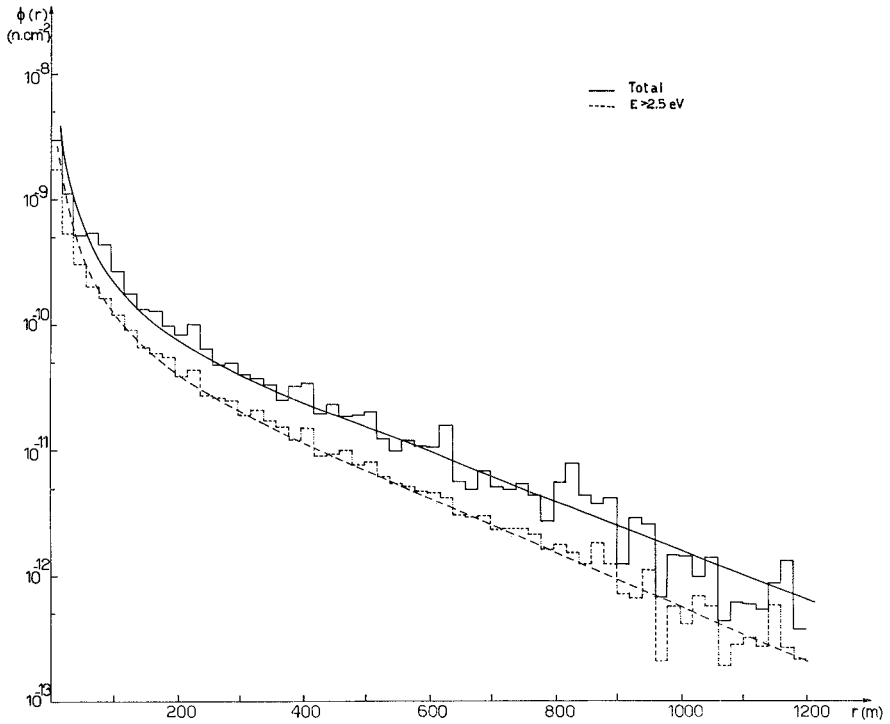

Fig. 2. Neutron fluence as a function of the distance from the source, with $\theta = 60°$.

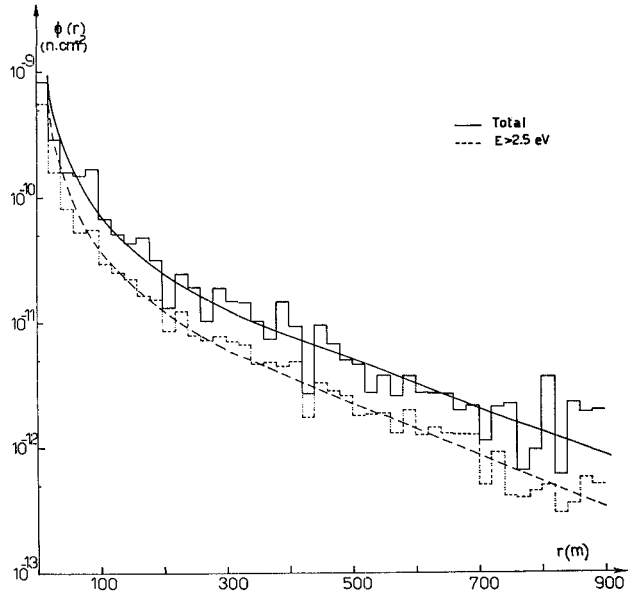

Fig. 3. Neutron fluence as a function of the distance from the source, with $\theta = 30°$.

TABLE 2
Values of the parameter a.

Na	Mg	Al	Si	K	Ca	Fe
0.37	0.39	0.45	0.45	0.50	0.90	1.70

and carbon do not follow this rule. For these elements we used experimental data[8]).

Capture: All the processes, (n,α), (n,γ), (n,p), etc., in which there are no neutrons in the final state have been considered as capture reactions.

The capture cross section $\sigma_c(E)$ has been deduced from experimental data using the relation:

$$\sigma_c(E) = \sigma_n(E) - \sigma_{n'}(E).$$

3.2. $E < 0.2$ eV

When the neutron energy becomes less than 0.2 eV one must also take into account the motion of the nuclei.

For such a neutron only elastic interactions and capture have been considered.

Instead of the energy of the neutron, we used the corresponding velocity v ($v = 1.383 \times 10^6 E^{\frac{1}{2}}$ cm/s, with E in eV). A maxwellian velocity distribution for the interacting nuclei has been used.

Reciprocal interactions between atoms have been neglected.

In these conditions, the probability for a neutron with velocity v to interact with a nucleus with a velocity lying between w and $w+\mathrm{d}w$ and with a relative direction lying between μ and $\mu+\mathrm{d}\mu$ (μ is the cosine of the angle between the velocities) is [9]):

$$R(w,\mu|v)\mathrm{d}w\,\mathrm{d}\mu = 4\pi N_i(\alpha_i/\pi)^{\frac{3}{2}}\{\exp(-\alpha_i w^2)\}w^2 \cdot \cdot|\boldsymbol{v}-\boldsymbol{w}|\{\sigma_{is}+(B_i/v)\}^{\frac{1}{2}}\mathrm{d}w\,\mathrm{d}\mu,$$

where $\alpha_i = \frac{1}{2}M_i/(kT)$, M_i being the mass of the i^{th} element and N_i its concentration, k Boltzmann's constant, T the room temperature (in °K), σ_{is} and B_i/v [4]) the microscopic diffusion cross section and the capture cross section respectively for the i^{th} element.

The velocity v' of the neutron after collision is:

$$v' = \{\beta^2|\boldsymbol{v}-\boldsymbol{w}|+g^2+2\beta|\boldsymbol{v}-\boldsymbol{w}|g\lambda\}^{\frac{1}{2}},$$

where $\beta = A_i/(A_i+1)$, A_i being the atomic number of the element, g the center of mass velocity and λ the cosine of the diffusion angle in the CM system.

The elastic diffusion has been considered to be isotropic in the CM system.

4. Results

The results of our computation are shown in figs. 1–3, the histograms representing respectively the three cases considered. The neutron fluence per primary neutron is represented as a function of the distance from the source. θ is the semi-aperture angle of the neutron emission cone.

TABLE 3
Number of neutrons per primary neutron ($\theta = 90°$).

	$0 < r < 100$ (m)	$100 < r < 300$ (m)	$300 < r < 600$ (m)	$600 < r < 1000$ (m)	$r > 1000$ (m)
$E < 0.2$ eV	1.63×10^{-1}	2.37×10^{-1}	1.65×10^{-1}	9.36×10^{-2}	2.07×10^{-2}
0.2 eV $< E <$ 10 keV	8.66×10^{-2}	1.27×10^{-1}	1.01×10^{-1}	5.69×10^{-2}	1.43×10^{-2}
10 keV $< E <$ 100 keV	5.95×10^{-3}	1.47×10^{-2}	1.63×10^{-2}	8.25×10^{-3}	2.88×10^{-3}
100 keV $< E <$ 1 MeV	1.82×10^{-2}	3.59×10^{-2}	3.97×10^{-2}	2.05×10^{-2}	5.50×10^{-3}
1 MeV $< E <$ 2 MeV	1.26×10^{-2}	3.11×10^{-2}	3.06×10^{-2}	1.25×10^{-2}	2.30×10^{-3}
2 MeV $< E <$ 3 MeV	1.98×10^{-2}	4.47×10^{-2}	3.03×10^{-2}	1.06×10^{-2}	1.21×10^{-3}
3 MeV $< E <$ 4 MeV	6.95×10^{-2}	7.29×10^{-2}	2.77×10^{-2}	6.72×10^{-3}	7.04×10^{-4}
4 MeV $< E <$ 5 MeV	1.06×10^{-1}	8.54×10^{-2}	2.84×10^{-2}	5.31×10^{-3}	2.56×10^{-4}

TABLE 4
Number of neutrons per primary neutron ($\theta = 60°$).

	$0 < r < 100$ (m)	$100 < r < 300$ (m)	$300 < r < 600$ (m)	$600 < r < 1000$ (m)	$r > 1000$ (m)
$E < 0.2$ eV	7.86×10^{-2} 1.64×10^{-1}	9.19×10^{-2} 1.93×10^{-1}	6.58×10^{-2} 1.38×10^{-1}	4.15×10^{-2} 8.71×10^{-2}	7.10×10^{-3} 1.49×10^{-2}
0.2 eV $< E <$ 10 keV	3.82×10^{-2} 8.01×10^{-2}	5.04×10^{-2} 1.05×10^{-1}	4.62×10^{-2} 9.69×10^{-2}	2.48×10^{-2} 5.21×10^{-2}	5.76×10^{-3} 1.20×10^{-2}
10 keV $< E <$ 100 keV	2.30×10^{-3} 4.83×10^{-3}	5.95×10^{-3} 1.24×10^{-2}	7.93×10^{-3} 1.66×10^{-2}	4.28×10^{-3} 9.00×10^{-3}	1.21×10^{-3} 2.55×10^{-3}
100 keV $< E <$ 1 MeV	7.36×10^{-3} 1.54×10^{-2}	1.63×10^{-2} 3.42×10^{-2}	1.78×10^{-2} 3.74×10^{-2}	9.47×10^{-3} 1.98×10^{-2}	3.00×10^{-3} 6.31×10^{-3}
1 MeV $< E <$ 2 MeV	4.73×10^{-3} 9.94×10^{-3}	1.37×10^{-2} 2.88×10^{-2}	1.45×10^{-2} 3.04×10^{-2}	6.27×10^{-3} 1.31×10^{-2}	1.34×10^{-3} 2.82×10^{-3}
2 MeV $< E <$ 3 MeV	9.47×10^{-3} 1.98×10^{-2}	2.18×10^{-2} 4.59×10^{-2}	1.33×10^{-2} 2.80×10^{-2}	4.60×10^{-3} 9.67×10^{-3}	5.12×10^{-4} 1.07×10^{-3}
3 MeV $< E <$ 4 MeV	3.48×10^{-2} 7.32×10^{-2}	2.90×10^{-2} 6.08×10^{-2}	1.14×10^{-2} 2.40×10^{-2}	2.24×10^{-3} 4.70×10^{-3}	3.20×10^{-4} 6.71×10^{-4}
4 MeV $< E <$ 5 MeV	3.18×10^{-2} 6.67×10^{-2}	1.94×10^{-2} 4.08×10^{-2}	5.18×10^{-3} 1.08×10^{-2}	9.60×10^{-4} 2.01×10^{-3}	6.40×10^{-5} 1.34×10^{-4}

TABLE 5
Number of neutrons per primary neutron ($\theta = 30°$).

	$0 < r < 100$ (m)	$100 < r < 300$ (m)	$300 < r < 600$ (m)	$600 < r < 100$ (m)	$r > 1000$ (m)
$E < 0.2$ eV	2.56×10^{-2} 1.66×10^{-1}	2.84×10^{-2} 1.85×10^{-1}	2.09×10^{-2} 1.35×10^{-1}	1.38×10^{-2} 9.01×10^{-3}	4.48×10^{-4} 2.92×10^{-3}
0.2 eV $< E <$ 10 keV	1.07×10^{-2} 7.01×10^{-2}	1.25×10^{-2} 8.18×10^{-2}	1.54×10^{-2} 1.00×10^{-1}	8.19×10^{-3} 5.34×10^{-3}	8.32×10^{-4} 5.42×10^{-3}
10 keV $< E <$ 100 keV	5.12×10^{-4} 3.33×10^{-4}	1.72×10^{-3} 1.12×10^{-2}	2.49×10^{-3} 1.62×10^{-2}	1.53×10^{-3} 1.00×10^{-2}	1.28×10^{-4} 8.34×10^{-4}
100 keV $< E <$ 1 MeV	1.47×10^{-3} 9.59×10^{-3}	4.73×10^{-3} 3.08×10^{-2}	5.50×10^{-3} 3.58×10^{-2}	3.39×10^{-3} 2.21×10^{-2}	5.76×10^{-4} 3.75×10^{-3}
1 MeV $< E <$ 2 MeV	1.60×10^{-3} 1.04×10^{-2}	4.86×10^{-3} 3.17×10^{-2}	4.60×10^{-3} 3.00×10^{-2}	1.72×10^{-3} 1.12×10^{-2}	5.76×10^{-4} 3.75×10^{-3}
2 MeV $< E <$ 3 MeV	3.32×10^{-3} 2.17×10^{-2}	7.61×10^{-3} 4.96×10^{-2}	4.48×10^{-3} 2.92×10^{-2}	1.28×10^{-3} 8.34×10^{-3}	6.40×10^{-5} 4.17×10^{-4}
3 MeV $< E <$ 4 MeV	1.16×10^{-2} 7.59×10^{-2}	7.29×10^{-3} 4.75×10^{-2}	3.84×10^{-3} 2.50×10^{-2}	6.40×10^{-4} 4.17×10^{-3}	6.40×10^{-5} 4.17×10^{-4}
4 MeV $< E <$ 5 MeV	8.38×10^{-3} 5.46×10^{-2}	3.84×10^{-3} 2.50×10^{-2}	9.60×10^{-4} 6.26×10^{-3}	1.28×10^{-4} 8.34×10^{-4}	– –

There are two histograms in each figure, the one representing the total neutron fluence, and the other the fluence for neutrons of energy greater than 2.5 eV. This distinction has been made because usually, in the dose measurements in the vicinity of the accelerators, the detectors are covered with a suitable cadmium thickness to eliminate neutrons with energies less than 2.5 eV, whose contribution to the dose is negligible.

Table 3 shows the number of neutrons per primary neutron with energy in the considered intervals, at various distances from the source, with $\theta = 90°$.

The case $\theta = 60°$ is shown in table 4. In this case, for each zone and for each energy interval, two numbers are given: the first gives the ratio between scattered neutrons and primary neutrons emitted from the source over the whole solid angle; the second shows the ratio between scattered neutrons and primary neutrons emitted in the considered angle.

The corresponding results for $\theta = 30°$ are shown in table 5.

5. Analysis of the results

In figs. 1–3 the best fitting curves for the results are drawn.

They can be represented by the relation:

$$\phi(r) = Ar^{-\alpha}, \qquad (1)$$

for values of r between 20 m and 300 m, where ϕ is the neutron fluence and r the distance from the source.

For r greater than 300 m, the relation becomes

$$\phi(r) = B\exp(-r/\lambda). \qquad (2)$$

The values of A, B, α and λ are given in table 6 for the curves relating to the total neutron fluence and in table 7 for those relating to neutrons with energy greater than 2.5 eV.

The constants A and B depend only on the intensity and geometry of the source.

TABLE 6

θ	A	B	α	λ(m)
30°	8.24×10^{-8}	4.75×10^{-11}	1.53	232
60°	3.56×10^{-7}	1.50×10^{-10}	1.59	220
90°	6.03×10^{-7}	5.25×10^{-10}	1.47	200

TABLE 7

θ	A	B	α	λ(m)
30°	8.45×10^{-8}	2.40×10^{-11}	1.67	215
60°	2.33×10^{-7}	8.75×10^{-11}	1.63	200
90°	5.17×10^{-7}	3.30×10^{-10}	1.57	180

Instead, the exponent α appearing in eq. (1) is independent of the source geometry, but depends only on the energy of the neutrons.

We can indeed assume, within 6%, $\alpha = 1.5$ for the curves relating to the total neutron fluence and $\alpha = 1.6$ for the curves relating to the fluence of neutrons with energy greater than 2.5 eV.

These values for α are in very good agreement with the results of the skyshine measurements at CERN [10]).

At distances greater than 300 m it seems that the simple exponential law of eq. (2) holds, where λ can be assumed as the mean free path for diffusion. λ also seems to depend on the energy although not very strongly, since, within 10%, we can assume $\lambda = 220$ m for the curves relating to table 6 and $\lambda = 200$ m for those related to table 7.

These values are not very different from those used by Lindenbaum[2]), 138 m for neutrons of energy between 1 MeV and 5 MeV, by Williams[2]) 270 m for neutrons of energy between 5 MeV and 10 MeV, and by Panofsky[2]), 305 m.

Fig. 1 also shows the curve predicted by the Lindenbaum theory[2]). As one can see, the agreement with our results is very good, so the numerous experimental confirmations of the Lindenbaum theory can be considered as a proof at the correctness of our calculation.

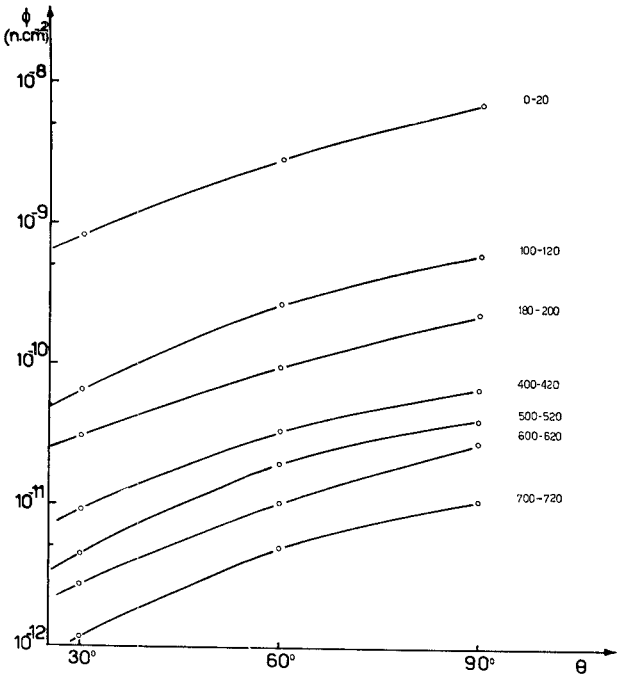

Fig. 4. Neutron fluence as a function of θ, at various distances from the source.

The effect of the lateral shields on the skyshine intensity can be deduced from the decreasing of the coefficients A and B with decreasing angle θ in tables 6 and 7.

The effect is even more evident in fig. 4, where the total neutron fluence is given as a function of θ for various distances from the source.

As one can see, the presence of lateral shields, provided they are in the close vicinity of the machines, can strongly reduce the skyshine intensity, often substituting the lack of an efficient overhead screen.

We also note that the lateral shields notably modify the energy spectrum of diffused neutrons, as one can see in tables 3–5.

Finally, the ratio between the reflected and incident neutrons allowed us to obtain the back scattering coefficient of the earth's surface. It turned out to be about 0.61 for the considered source, in very good agreement with previous values, which were all within 0.5 and 0.8 for neutrons of energy between 1 MeV and 10 MeV [1]).

6. Conclusions

As a conclusion, the results of our calculation seem to be very satisfactory especially in relation with the Lindenbaum theory, which agrees with numerous measurements.

Further, our formulas seem to be very simple to use and one can take the lateral shields into account only by a suitable choice of the coefficients.

References

1) M. S. Livingston and J. P. Blewett, *Particle accelerators* (McGraw-Hill, 1962).
2) S. J. Lindenbaum, USAEC no. TID-7545 (1957).
3) R. J. Howerton, UCRL 5351 (1958).
4) D. J. Hughes and J. A. Harvey, Neutron cross sections, BNL-USAEC (1955).
5) E. Troubetzkoy, M. Kalos and H. Lustig, Neutron Cross Sections, NDA 2111 (1959).
6) J. B. Marion and J. L. Fowler, *Fast neutron physics* (Marshak, 1963).
7) M. D. Goldberg, V. M. May and J. R. Sthen, BNL-400 (1962).
8) B. T. Price, C. C. Horton and K. T. Spinney, *Radiation shielding* (Pergamon Press, 1957).
9) R. R. Coveyou, R. R. Bate and R. K. Osborne, Effect of moderator temperature upon neutron flux in infinite capturing medium, ORNL (1958).
10) A. Rindi and J. Baarli, CERN Int. Rep. DI/HP/19 (1963).